Stability assessment of masonry arches by evolutionary fracturing process analysis

Stability assessment of masonry arches by evolutionary fracturing process analysis

Federico Accornero[1], Giuseppe Lacidogna[1], Stefano Invernizzi[1], Alberto Carpinteri[1]
[1]*Department of Structural, Geotechnical and Building Engineering, Politecnico di Torino, Italy*
E-mail: *federico.accornero@polito.it, giuseppe.lacidogna@polito.it, stefano.invernizzi@polito.it, alberto.carpinteri@polito.it*

Keywords: Arch structures, Fracture mechanics, Fracturing process, Crack opening and closure, Finite Element model.

ABSTRACT

Masonry arch structures, and, more in general, vaulted structures, are traditionally assessed using a well-established approach, such as linear elasticity or limit analysis, whereby system behaviour at the intermediate stage −that occurs when the material's tensile strength has been exceeded but the collapse mechanism has not yet formed− is disregarded. With an evolutionary fracturing process analysis for the stability assessment of a masonry arch it is possible to capture the damaging process that takes place when the conditions evaluated by means of linear elastic analysis no longer apply, and before the conditions assessed through limit analysis set in. Furthermore, the way the thrust line is affected by the opening of cracks and the redistribution of internal stresses can be checked numerically.

The evolutionary calculation method presented in this paper takes into account the intermediate cracking stage and uses a constitutive law providing a closer approximation to the actual behaviour of the structural material. By applying this numerical model the monumental arches of the Vittorio Emanuele I Bridge over the Po River, and the Mosca Arch Bridge over the Dora River both in Turin (Italy) are described. The different behaviors under increasing load of the two structural schemes –the Mosca Bridge is a very thin shallow masonry arch, while the Vittorio Emanuele I Bridge presents three-centered rounded arches– are deeply investigated by means of the evolutionary analysis.

NOTATION

A_i	cross-sectional area of the i-th segment of the arch
a	crack depth

b	section width
E	Young's modulus
e	axial force eccentricity with respect to the section centroid
F_i	axial force applied to the i-th arch segment
F_0	axial force due to the real load acting on the arch
F_1	axial force due to horizontal fictitious force X_1=1
I_i	moment of inertia of the i-th arch segment
K_I	stress intensity factor
K_{IC}	fracture toughness
l	beam finite element length
L_{tot}	arch total strain energy
L_i	strain energy for each arch segment
M	bending moment
M_i	moment applied to the i-th arch segment
M_0	moment due to the real load acting on the arch
M_1	moment due to horizontal fictitious force X_1=1
M_2	moment due to fictitious moment X_2=1
t	section thickness
X_1, H	unknown axial force applied to the crown of the arch
X_2, B	unknown moment applied to the crown of the arch
Δs	arch segment
ξ	normalized crack depth
ξ^*	normalized closure depth

INTRODUCTION

Albeit well-established, the linear elastic and/or limit analysis approaches traditionally employed to assess the behaviour of arch structures, and, more in general, vaulted structures, often leave the structural engineer at a loss (Page 1993). While linear elastic analysis is applicable when the thrust line stays within the central kern to prevent tension arising, and not to exceed the limits of elastic theory, limit analysis gives a thrust line, between hinges, which lies everywhere within the masonry of the arch ring. Therefore, neither analysis can capture the intermediate damaging stage, which occurs during the loading process, immediately before and after the conditions addressed by the previous schemes. In other words, whereas linear elastic analysis can describe a structure up to the onset of the first non-linearities, limit analysis defines the ultimate conditions prior to the final collapse, produced when the thrust line is tangent at least four times – four hinges– to the arch edges. There is a need for a more sophisticated

computational method that uses a real constitutive law of the material, and enables the cracking stages between elastic behaviour and final collapse to be taken into account (Lourenço 2000, Zucchini and Lourenço 2000). Such a method is introduced in this work by adopting an elastic-softening schematization for masonry and, more generally, for quasi-brittle materials. As Hillerborg has shown (Hillerborg et al. 1976), considering an elastic-softening constitutive law for the material is equivalent to employing an elastic constitutive law coupled with a fracture process according to Linear Elastic Fracture Mechanics (LEFM) concepts.

The opening of cracks in elastic-softening structures is believed to affect the thrust line to modify the static behaviour of the structures and to redistribute the internal stresses; similarly, elasto-plastic frame structures are believed to profit from the formation of plastic hinges. The aim of this study was to address the problems associated with the softening and cracking process in masonry arches; to this end, a discrete model of the Mosca arch bridge over the Dora river in Turin was developed using beam finite elements, and a step-by-step loading process was applied in analogy with Castigliano's analysis (Castigliano 1879). For each loading increment, the axial force and the bending moment at the ends of each beam element were computed. Based on such values, a check against crushing and tensile failure was performed. When a crushing crisis occurs, this is considered final for the arch section, while in the case of a local tensile failure the routine simulates the formation of a crack and introduces an elastic hinge of suitable stiffness. Crack depth is determined according to LEFM concepts (Broek 1984; Carpinteri 1992; Carpinteri et al. 1982; Milne et al. 2003): it stabilizes at a value which is a function of the axial force and its eccentricity, as well as of the geometric and mechanical characteristics of the cross-section. Based on crack depth, it is possible to compute the rotational stiffness of an elastic hinge simulating the crack; then, the local stiffness matrix of each individual cracked element is updated, and so is for the global stiffness matrix of the entire arch. The procedure takes into consideration the possibility of partial or total crack closure, during loading increments subsequent to the one that generated the crack.

STABILITY OF MASONRY ARCHES

Over the centuries, the evolution of masonry arch design methods has been addressed through a variety of critical approaches (Karnovsky 2012, Paradiso et al. 2007, Benvenuto and Radelet de Grave 1995; Page 1993); they are briefly described below in chronological order to show how a partial understanding of the structural behaviour of an arch, as can be garnered from traditional methods, may be effectively improved by an elastic-softening approach that takes the possibility of crack formation into due account.

For centuries, vaulted structures were dimensioned according to methods that relied solely on geometric parameters. While they provided an answer to the static problem, such methods originated from experience did not probe the intrinsic factors underlying the phenomena observed.

Design in its modern sense began in the eighteenth century, when De La Hire (1731) and Mascheroni (1785), among others, performed theoretical analyses and experimental tests to determine the state of an arch at final collapse (Benvenuto and Radelet de Grave 1995). The developed design philosophy is similar to the notions at the basis of modern limit state and plastic design (Fig. 1).

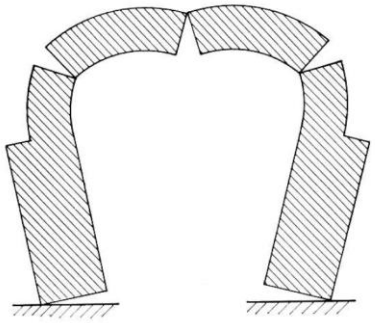

Figure 1. Collapse mechanism according to Mascheroni.

Navier (1839) was the first to make accurate observations on the distribution of stresses at the interfaces between the segments of an arch and to shift the focus of the analysis on the actual state of stress of the material. He introduced the thrust line concept to analyse stress distribution over a cross-section, and demonstrated that the resulting line of action had to lie within the central kern in order to prevent tension.

Mery's studies (1840) gained widespread recognition and were used extensively in the dimensioning of arch structures; his method used a graphic procedure to check the thrust line according to the limits identified by Navier.

The application of the theory of elasticity had some inevitable shortcomings in that the concepts of homogeneity and isotropy were totally disregarded.

Alberto Castigliano (1879) addressed the problem by applying the theorem of minimum strain energy to masonry arches, and introduced the "elastically imperfect system" concept: "*Les corps qui, après avoir été comprimés, ne reprennent pas exactement leur formes primitives en enlevants les forces extérieurs*" (Castigliano 1879).

In the famous example of iterative calculation applied to the arch of the Mosca Bridge over the Dora River in Turin (Castigliano 1879), Castigliano determined

the position of the thrust line by assuming the internal forces in the crown section to be unknown. The expression of deformation work was written by taking into account these unknown values while neglecting the contribution of shear. By imposing congruence conditions for the displacements in the crown section (i.e., assuming, by symmetry, rotation and horizontal displacements to vanish), the unknown parameters were determined by applying the energy theorem formulated by Castigliano himself. This also made it possible to determine the normal force and the bending moment for each section of the structure, the position of the neutral axis and hence the portion of the stress-carrying section under compression.

The stratagem to be adopted to verify the validity of the elastic hypotheses (especially the homogeneity of the material) consists of ensuring that the thrust line lies entirely within the middle third of the section, the presence of tension being incompatible with the nature of the material. Castigliano addressed this problem by resorting to the concept of an elastically imperfect system, whereby the elastic solution was worked out iteratively: the analysis was repeated so as to progressively reduce the parts in tension, and the initial dimensions of the model were modified at each step until the value obtained through subsequent approximations was deemed correct.

Starting from the assumption that "*the derivative of the complementary strain energy of a body with respect to a point load acting on that body is equal to the deflection, in the direction of the load, of the point on the body to which the load is applied*", Castigliano calculated the strain energy due to the contribution of the moment, M, and the axial force, F, for each of the segments, Δs, into which the arch was divided, each segment being characterized by cross-section, A, moment of inertia, I, and Young's modulus, E.

Considering the arch to be symmetrical, with fixed ends and the unknown X_1 and X_2 at the arch crown (Fig. 2), the total work, L_{tot}, was determined from the quantities calculated for the individual segment based on the unknown axial force and moment applied to the crown:

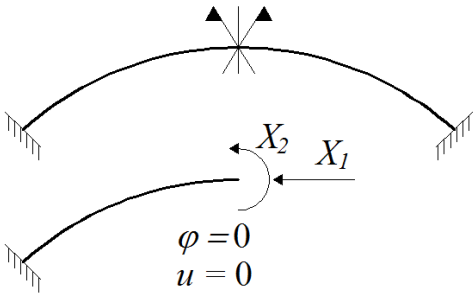

Figure 2. Schematic Mosca Bridge Arch Model from Castigliano's Analysis. X_1 is the unknown axial force applied to the crown of the arch; X_2 is the unknown bending moment applied to the crown of the arch; φ is the rotation of the arch crown and u is the horizontal displacement of the arch crown.

$$L_{tot} = \sum_{i=1}^{n} L_i \,, \tag{1}$$

$$L_i = \frac{1}{2E}\left(\frac{F_i^2}{A_i} + \frac{M_i^2}{I_i}\right)\Delta s \,, \tag{2}$$

with

$$F_i = F_0 + X_1 F_1 \,, \tag{3}$$

$$M_i = M_0 + X_1 M_1 + X_2 M_2 \,, \tag{4}$$

obtained by applying the Principle of Virtual Works. Thus, total work is given by the following expression:

$$L = \frac{1}{2}\frac{\Delta s}{E}\sum\left(\frac{(F_0 + X_1 F_1)^2}{A_i} + \frac{(M_0 + X_1 M_1 + X_2 M_2)^2}{I_i}\right). \tag{5}$$

Taking into account the congruence conditions −rotation and horizontal displacement of the arch crown equal to zero− and deriving by X_1 and X_2, respectively, we get:

$$\frac{\Delta s}{E}\left[X_1\sum\left(\frac{F_1^2}{A_i} + \frac{M_1^2}{I_i}\right) + X_2\sum\left(\frac{M_1 M_2}{I_i}\right) + \sum\left(\frac{F_0 F_1}{A_i} + \frac{M_0 M_1}{I_i}\right)\right] = 0 \,, \tag{6}$$

$$\frac{\Delta s}{E}\left[X_1\sum\left(\frac{M_1 M_2}{I_i}\right) + X_2\sum\left(\frac{M_2^2}{I_i}\right) + \sum\left(\frac{M_0 M_1}{I_i}\right)\right] = 0 \,, \tag{7}$$

from which it is possible to obtain the redundant unknowns X_1 and X_2. Once these values have been determined, the above expressions can provide all the necessary information regarding the stress state of each segment.

Castigliano also took into consideration the beneficial effects of the mortar beds interposed between the voussoirs of the Mosca Bridge in moving back the thrust line toward the centre line of the arch. He considered the energy applied by the axial force and bending moment on the prismatic shape of the mortar bed, defined a so-called "dragging work", which corrects the deformation work of the arch initially considered to consist exclusively of stone segments. Thus, the thrust line re-centring effect produced in the arch becomes evident.

The rigid blocks model used in the eighteenth century to study the behaviour of masonry arches underwent major revisions during the last century, based on several experiments carried out by Pippard (Page 1993; Pippard and Baker 1962) on arch models. One of the most significant revisions to eighteenth century theories was formulated by Heyman (Heyman 1966; Heyman 1969; Heyman 1982) who, referring back to Kooharian's studies (Kooharian 1953), proposed a systematic application of the limit analysis theorems to the problem of masonry arches stability in kinematic terms. Heyman introduced three basic assumptions for the application of limit analysis to masonry structures: "*stone has no tensile strength; stone has infinite compressive strength; the sliding of a stone on another cannot occur"*.

The choice of this constitutive law for the material appears penalising compared to the actual behaviour of the material: even if we admit that the shear component of the stress exerted between two adjacent voussoirs can never exceed the friction between them, we are still dealing with a material having no tensile strength and infinite compressive strength.

Starting from these assumptions, it is possible to admit the formation of a hinge where the line of thrust is tangent to the edges of an arch: a rigid rotation of the two adjacent segment faces occurs around the extreme fibre of the section (Orduna and Lourenço 2001).

Three tangential points give rise to the formation of three hinges, resulting in a statically determinate structure; the limit for triggering a kinematic collapse mechanism is the formation of a fourth hinge. Thus, limit analysis consists of identifying the smallest possible load system generating a line of thrust that is always contained within the volume of the arch and tangent to arch edges at four points (Fig. 3).

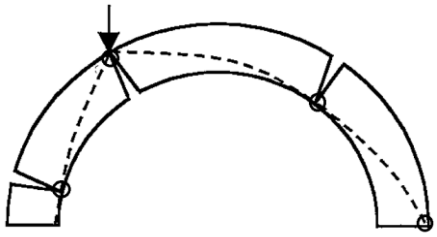

Figure 3. Collapse mechanism due to the formation of four hinges.

The finite element analysis of arch and shell structures has been studied extensively, and numerous studies, from the earliest by Towler and Sawko to the most recent (Choo et al. 1991; Crisfield and Wills 1986; Towler and Sawko 1982), show the potential of the finite elements method for computing load-deflection curves (Giambanco et al. 2000) and the interaction with the filling. We should also mention recent methods for the assessment of the stability of masonry arch structures consisting of structural monitoring by means of the Acoustic Emissions Technique (Carpinteri et al. 2007; Invernizzi et al. 2010).

FRACTURING PROCESS IN MASONRY ARCHES

Constitutive law

Masonry is characterised by anisotropic and non-linear behaviour even at low strain values (Berto et al. 2002). Masonry materials subject to uniaxial load tests exhibit appreciably different tensile strength and compressive strength values: the latter being significantly higher than the former.

The constitutive law that best represents the behaviour of natural or artificial masonry materials is an elastic-softening constitutive law (Fig. 4). This is equivalent to simply considering an elastic constitutive law combined with a crisis condition for fracturing in accordance with the concepts of LEFM; that is to say, the material has a purely elastic behaviour with the possibility of cracks forming and propagating.

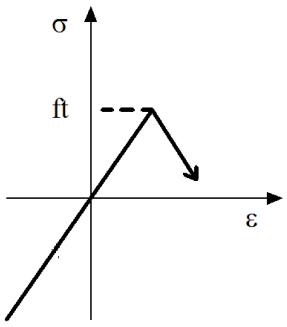

Figure 4. Elastic-softening constitutive law.

Mechanism of crack opening and closure

As anticipated, the elastic-softening material is replaced by a material with a purely elastic behaviour with the possibility of cracks formation and extension. This hypothesis applies only to structures large enough to allow tension profiles to develop close to the crack tip, as foreseen by Linear Elastic Fracture Mechanics.

Let us take normalized crack depth $\xi = a/b$ (Fig. 5a) as damage parameter, and the stress intensity factor, K_I, (Fig. 5b) as load parameter. The stress intensity factor is an amplification factor of the stress field when the loads are symmetrical relative to the crack (e.g. axial force and bending moment) (Carpinteri 1982; Murakami 1987; Tada et al. 1985). Shear is disregarded.

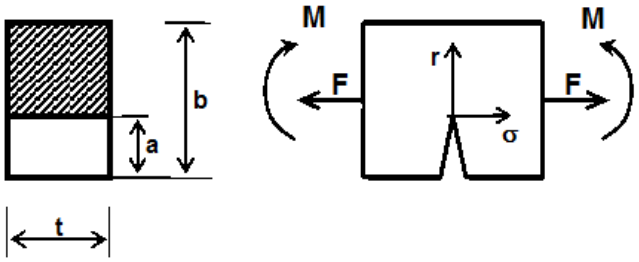

Figure 5. Cracked beam element: $\xi = ab^{-1}$; $\sigma = K_I(2\pi r)^{-0.5}$.

It is interesting to remember the energetic meaning of K_I: the square of this parameter –omitting a proportionality factor– represents the elastic energy released by the system per unit of virtual crack extension. K_I reaches its critical value K_{IC} when this virtual extension becomes real, since the energy released in an elementary crack extension is sufficient to supply the surface energy of the new geometry (Irwin 1957; Carpinteri 1982; Murakami 1987; Tada et al. 1985).

The bending moment produces a stress intensity factor at the crack tip, expressed as (Murakami 1987; Tada et al. 1985):

$$K_I = \frac{M}{tb^{\frac{3}{2}}} Y_M(\xi), \tag{8}$$

with

$$Y_M(\xi) = 6\left(1.99\xi^{\frac{1}{2}} - 2.47\xi^{\frac{3}{2}} + 12.97\xi^{\frac{5}{2}} - 23.17\xi^{\frac{7}{2}} + 24.8\xi^{\frac{9}{2}}\right). \tag{9}$$

Similarly, a tensile axial force, F, produces (Murakami 1987; Tada et al. 1985):

$$K_I = \frac{F}{tb^{\frac{1}{2}}} Y_F(\xi), \tag{10}$$

with

$$Y_F(\xi) = 1.99\xi^{\frac{1}{2}} - 0.41\xi^{\frac{3}{2}} + 18.70\xi^{\frac{5}{2}} - 38.50\xi^{\frac{7}{2}} + 53.86\xi^{\frac{9}{2}}. \tag{11}$$

When the axial force is compressive and the bending moment tends to open the crack, as is usually the case in masonry arches, the total stress intensity factor can be determined by applying the Superposition Principle:

$$K_I = K_{IM} - K_{IF} = \frac{F}{tb^{\frac{1}{2}}}\left[\frac{e}{b} Y_M(\xi) - Y_F(\xi)\right], \tag{12}$$

where *e* stands for the eccentricity of the equivalent axial force, relative to the centroid of the cross-sectional area.

From the critical condition $K_I = K_{IC}$, it is possible to determine the dimensionless crack extension axial force as a function of crack depth ξ and relative eccentricity of the load, *e/b*:

$$\overline{F}_C = \frac{F_C}{tb^{\frac{1}{2}} K_{IC}} = \frac{1}{\frac{e}{b} Y_M(\xi) - Y_F(\xi)}. \tag{13}$$

The curves in Fig. 6 graphically represent this expression and show how, when eccentricity *e/b* is fixed, the fracturing process reaches a condition of stability only after showing an unstable condition. If the load *F* is unable to follow the decreasing unstable branch of the *e/b = constant* curve in a *"strain-softening"* unloading process, the fracturing process leads to catastrophic behaviour and the representative point advances horizontally until it meets the *e/b = constant* curve again on the stable branch. On the other hand, the possibility of load relaxation and a more or less catastrophic fracturing behaviour depends on the structure's geometric and mechanical characteristics and is affected in particular by degree of redundancy and size (scale effect) (Carpinteri 1992).

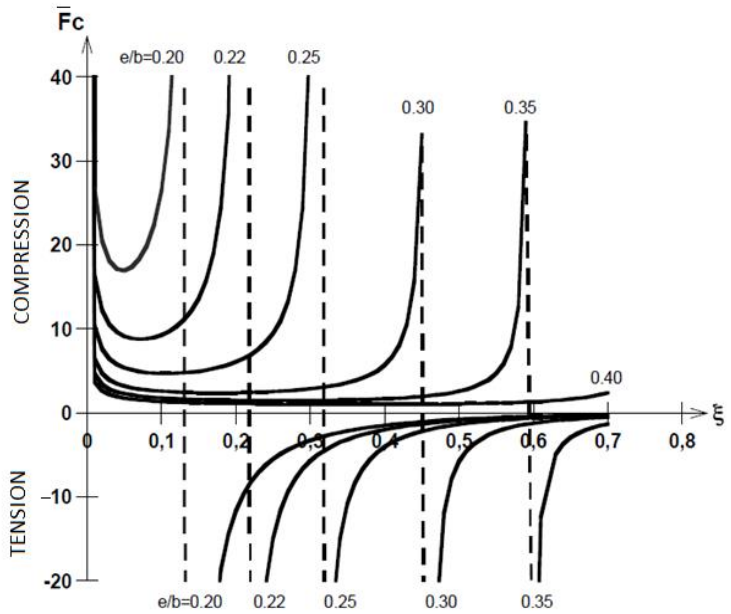

Figure 6. Fracturing process for eccentric axial load.

It is also important to consider that, for each relative crack depth ξ, there is a relative eccentricity value below which the crack tends, at least partially, to close again. From the closing condition $K_I = 0$, we get:

$$K_I = 0 = \frac{F}{tb^{\frac{1}{2}}}\left[\frac{e}{b}Y_M(\xi) - Y_F(\xi)\right], \tag{14}$$

from which:

$$\frac{e}{b} = \frac{Y_F(\xi)}{Y_M(\xi)}. \tag{15}$$

Equation (15) is graphically represented in Fig. 7. The area below the curve represents the crack and loading conditions whereby $K_I < 0$.

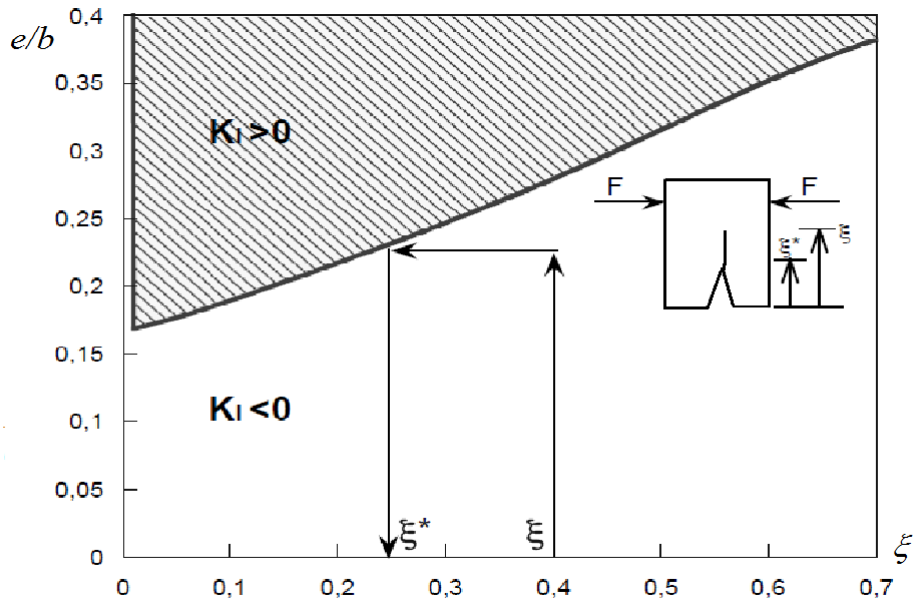

Figure 7. Crack closure curve.

Stiffness of the cracked section

Let us now consider the loss of stiffness in the cross-section of a cracked beam. A cracked cross-section (Fig.5a) behaves like an elastic hinge with the rotational stiffness determined by an energy balance between elastic work and fracture work (Carpinteri 1983; Chondros and Dimarogonas 1998; Krawczuk et al. 2000; Okamura et al. 1975; Parmerter 1976).

The rotational stiffness of an elastically fixed joint is:

$$W = \frac{b^2 tE}{2\int_0^{\xi} Y_M^2(\xi)\,\mathrm{d}\xi}, \tag{16}$$

where E is the Young's modulus of the material.

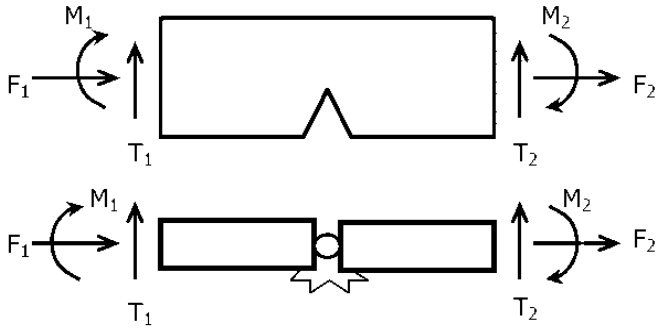

Figure 8. Cracked beam element: elastic hinge simulating a crack.

The stiffness matrix of the cracked element (Fig.8) is changed only by the four rotational terms as follows (Carpinteri 1983; Chondros and Dimarogonas 1998; Krawczuk et al. 2000; Okamura et al. 1975; Parmerter 1976):

	u_1	v_1	φ_1	u_2	v_2	φ_2
F_1	$\frac{EA}{l}$	0	0	$-\frac{EA}{l}$	0	0
T_1		$12\frac{EI}{l^3}$	$-6\frac{EI}{l^2}$	0	$-12\frac{EI}{l^3}$	$-6\frac{EI}{l^2}$
M_1			$\frac{EI(3EI+4lW)}{l(EI+lW)}$	0	$6\frac{EI}{l^2}$	$\frac{EI(3EI+2lW)}{l(EI+lW)}$
F_2				$\frac{EA}{l}$	0	0
T_2			SYMMETRIC		$12\frac{EI}{l^3}$	$6\frac{EI}{l^2}$
M_2						$\frac{EI(3EI+4lW)}{l(EI+lW)}$

where A and I are the area and the inertia moment of the cross-section, respectively, and l is the length of the beam finite element.

From the stiffness matrix, it can be seen that terms which link the moments M_1 and M_2 to the rotations φ_1 and φ_2, obtained by applying the Principle of Virtual

Work to a beam with an elastic hinge simulating a crack at the midspan, return the standard values of the uncracked beam finite element as W tends to infinity:

$$\lim_{W\to\infty} \varphi \frac{EI\left(3EI+4lW\right)}{l\left(EI+lW\right)} = \varphi \frac{4EI}{l}, \tag{17}$$

$$\lim_{W\to\infty} \varphi \frac{EI\left(3EI+2lW\right)}{l\left(EI+lW\right)} = \varphi \frac{2EI}{l}. \tag{18}$$

Calculation procedure

Setting the geometrical characteristics of the structure and the mechanical characteristics of the material, like the maximum compressive stress and the fracture toughness K_{IC}, the arch is analysed by creating a FEM model and considering the stone structure clamped to rigid abutments. The calculation uses a step-by-step loading process, and for each load increment the code returns the axial force and bending moment in each section; from these values, using the classical relations of beam theory, it is possible to determine the maximum tensile or compressive forces and their eccentricity with respect to the centroid in each section of the structure.

When a section crisis is triggered by tensile stresses, the relative crack depth ξ is determined from eq.13, that gives the relation between the crack depth ξ and the relative eccentricity e/b of the axial force. In this way the updated crack depth is determined. For this equation some dimensionless curves are shown in Fig.6.

Therefore, the routine is applied again considering the modified stiffness of the cracked elements (see eq.16). If the new relative crack depth ξ is equal to that formerly determined, the process stabilizes. If the new relative crack depth ξ is lower than the former, the routine resorts to the "curve of closure" (see eq.15), which allows to check the value of the stress intensity factor K_I, determining the admissible crack depth. After this check, the ξ values which fall in the field $K_I \geq 0$ (see Fig.7) are considered.

Increasing the load, the inefficiency of the arch section takes place when $\xi \geq 0.7$ [UIC 1995], or when the compressive strength in the considered element is reached.

NUMERICAL APPLICATIONS

Mosca bridge

An application of the aforementioned evolutionary method to a masonry arch bridge (Fig. 9) designed by Carlo Bernardo Mosca (1792-1867) is described

below and then compared with the iterative analysis carried out by Alberto Castigliano (1879) on the same bridge.

Mosca Bridge, inaugurated in 1830, still spans the Dora river in Turin (Fig. 10,11). This shallow stone arch bridge is unanimously recognized as a pioneering work and, at the same time, as a milestone in the history of stone bridge construction (Chiorino et al. 2001). The importance of the bridge lies both in the innovative design and construction techniques adopted by Mosca and in its outstanding geometrical characteristics (see Table 1). The arch bridge masonry fabric consists of 93 granite segments.

Figure 9. Original structural model of the Mosca Bridge (19th century), Department of Structural, Geotechnical & Building Engineering, Politecnico di Torino (Italy).

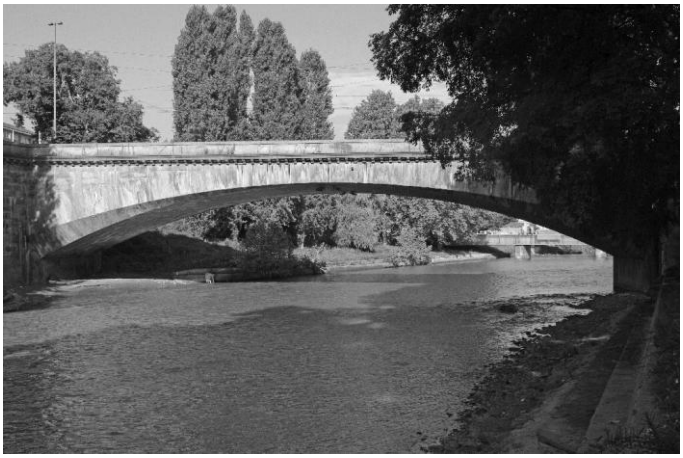

Figure 10. Mosca Bridge over the Dora River in Turin, Piedmont (Italy).

Figure 11. Mosca Bridge under Service Loads.

Table 1. Mosca Bridge geometrical characteristics.

Span	**Rise**	**Radius**	**Arch Angle**	**Crown Depth**	**Springing Depth**	**Total Width**
45.00 m	5.50 m	48.80 m	54°56’42’’	1.50 m	2.00 m	12.60 m

Mosca Bridge iterative analysis by Castigliano

Castigliano, based on the geometry of the Mosca Bridge (Fig. 12), considered the loads on a strip of the bridge, of unit width, to consist of the segments weight (Manalaggio Granite: 27.50 kNm^{-3}), the filling weight (23.00 kNm^{-3}), and an evenly distributed live load of 6.00 kNm^{-2} (Castigliano 1879). Considering the arch to be symmetrical, Castigliano divided one half of the structure into six segments of equal length, each loaded by the respective segments weight, filling weight and live loads.

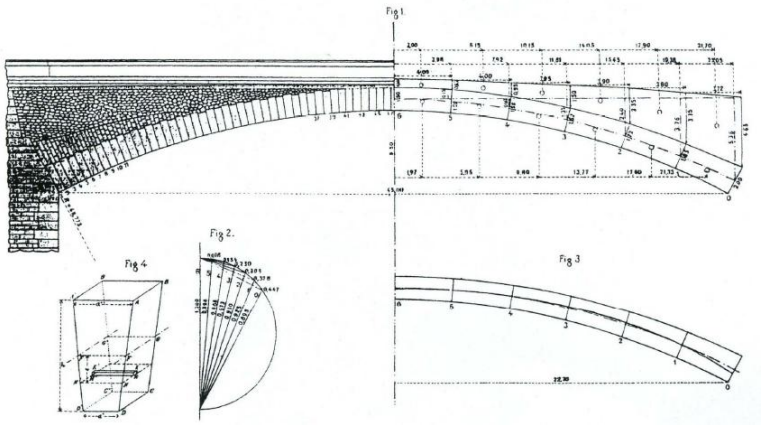

Figure 12. Geometric scheme of Mosca Bridge by Castigliano.

Applying the procedure described above, the iterative analysis of Castigliano is summarized as follows.

(i) By taking the horizontal thrust, $H = X_1$, the bending moment, $B = X_2$, and disregarding the presence of mortar joints, from the first iteration, we get $B = -218.00$ kNm (negative moment, which puts the intrados under tension according to Castigliano's reference system) and $H = 3247.10$ kN. Hence, at the springings we have $B_0 = 2597.37$ kNm, and $H_0 = 3928.27$ kN.

The resultant eccentricity at the springing, relative to the section centroid, is $B_0/H_0 = 0.66$ m, a value larger than the depth of the section divided by six (2.00/6 = 0.33 m). For this reason, the thrust line is outside the central kern.

Applying the Navier equation, the depth of the section in compression would be 1.51 m from the intrados, and the depth of the reduced part would be 0.49 m from the extrados. It is therefore necessary to identify the actual stress-carrying section, smaller than its apparent size, through subsequent approximations.

To determine the actual position of the thrust line, the stress-carrying section at the springings is now assumed to be as deep as the part determined to be in compression in the previous calculation, i.e., 1.51 m. For all the remaining sections, the entire depth is considered, since the eccentricity of the axial force is always smaller than the depth of the totally compressed section divided by six.

(ii) Repeating the procedure described in Section 2, from the second iteration we obtain the following values: $B = -111.20$ kNm, and $H = 3339.60$ kN in the crown; and at the springings: $B_0 = 1221.66$ kNm, and $H_0 = 4038.32$ kN.

With these values, eccentricity at the springings is $B_0/H_0 = 0.30$ m, a value which is still larger than the depth of the stress-carrying section divided by six (1.51/6 = 0.25 m). It follows that, near the springings, the line of thrust still remains outside of the central kern.

The depth of the compressed section now is 1.37 m from the intrados; and hence the reduced part is 0.13 m.

(iii) Then, Castigliano's procedure presents a third iteration, using a proportionality relationship. The real compressed section at the springing is defined as $1.37 - x$, in which x is the final error of the calculation. By considering a starting depth at the springings of 2.00 m, the initial error is $2.00 - (1.37 - x) = 0.63 + x$. In the first iteration, a compressed section of 1.51 m is obtained, so that the error is $1.51 - (1.37 - x) = 0.14 + x$. In the second iteration, a compressed section 1.37 m deep is obtained, with an error x.

Assuming the initial errors to be proportional to the final errors, we can write:

$$(0.63 + x) : (0.14 + x) = (0.14 + x) : x, \qquad (19)$$

which gives $x = 0.05$. Then the depth of the real section will be $1.37 - 0.05 = 1.32$ m from the extrados, and hence the depth of the crack forming at the springings will be $2.00 - 1.32 = 0.68$ m. Since the thrust line at the springings now lies at the limit of the central kern of the real compressed section, the eccentricity of the axial force is $2.00/2 - 1.32/3 = 0.56$ m.

Mosca Bridge evolutionary analysis

With reference to the geometric parameters described above, for a bridge longitudinal segment of unitary width, we developed a FEM model consisting of 16 beam finite elements (Fig. 13), each 2.97 m in length, and having the geometric characteristics listed in Table 2 (the model was seen to be symmetrical).

The loads used in this study were the same as those considered by Castigliano. The loads related to each segment are summarized in Table 3.

Table 2. Geometrical properties of the Mosca Bridge beam finite elements.

Segment	**Inertia**	**Area**
	[m^4]	[m^2]
1	0.67	2.00
2	0.61	1.93
3	0.56	1.86
4	0.50	1.79
5	0.45	1.71
6	0.39	1.64
7	0.34	1.57
8	0.28	1.50

Table 3. Loads used in the analysis of Mosca Bridge.

Voussoir	**Segment Weight**	**Filling Weight**	**Live Load**	**Total**
	[kNm^{-1}]	[kNm^{-1}]	[kNm^{-1}]	[kNm^{-1}]
1	60.56	96.51	6.00	163.07
2	59.93	76.72	6.00	139.66
3	53.65	59.65	6.00	119.30
4	50.88	45.52	6.00	102.40
5	48.15	33.91	6.00	88.06
6	45.69	25.11	6.00	76.80
7	43.39	19.11	6.00	68.51
8	41.29	18.35	6.00	65.64

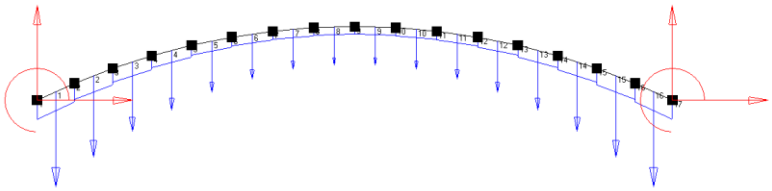

Figure 13. FEM calculation scheme of Mosca Bridge.

As described above, the bridge is composed of granite segments (Piedmont Manalaggio Granite) bonded with mortar beds. The system was assumed to have a compressive strength of 50 MPa, a tensile strength of 1.50 MPa, a Young's modulus of 50000 MPa, and a fracture toughness K_{IC} = 1.00 MN/m$^{3/2}$ (Bocca et al. 1989; Buyukozturk and Hearing 1998; Carpinteri 1981).

The loading process takes place in three steps, involving (i) the segments weight only, (ii) the segments weight and the filling weight, (iii) the segments weight, the filling weight and the live loads. The results are summarized in Table 4. The values refer to the sections at the springings, where the fracturing process occurs.

Table 4. Evolution of fracturing process in the structure of the Mosca Bridge.

Step	**Load Description**	**F_C**	**e**	**$\bar{F}_C$**	**e/b**	**ξ**	**ξ***
		[kN]	[m]	[-]	[-]	[-]	[-]
i	Segments Weight	2375.80	0.47	1.68	0.24	-	-
iia	Segments + Filling Weight	4025.51	0.67	2.85	0.33	0.45	-
iib	Segments + Filling Weight	4122.24	0.45	2.91	0.23	0.45	0.25
iic	Segments + Filling Weight	4059.60	0.59	2.87	0.30	0.27	-
iii	Segments W. + Filling W. + Live Load	4373.58	0.56	3.09	0.28	0.27	0.44

(i) It is evident that under the segments weight alone there is no fracturing of the arch.

(ii) The application of the filling weight triggers a fracturing process at the springings. The routine calculates $\bar{F}_C = 2.85$ and an initial crack depth $\xi = 0.45$ at the extrados, with $e/b = 0.33$. At this point, an elastic hinge of suitable stiffness is introduced in the cracked elements at the springings, i.e. the original structure assumes a lower global stiffness, and the calculation is repeated. We find $\bar{F}_C = 2.91$ and $e/b = 0.23$: the diagram of Fig.6 shows how, for such values, a crack depth ξ is not available.

Then the routine resorts to the "curve of closure" (Fig.7) that, for $e/b = 0.23$, gives $\xi^* = 0.25 < \xi = 0.45$. The calculation is repeated using the updated value ξ^*, because for $\xi = 0.45$, and $e/b = 0.23$, $K_I < 0$ is found (see Fig.7). From the calculation with $\xi = 0.25$, we find $\bar{F}_C = 2.87$, $e/b = 0.30$, and $\xi = 0.27$: therefore the crack stabilizes at $\xi = 0.27$.

(iii) Moreover, by adding the live loads to the dead ones, because of the modified stiffness, we get: $\bar{F}_C = 3.09$, $e/b = 0.28$, and $\xi = 0.17$ that is smaller than the previous crack depth $\xi = 0.27$. Then the routine resorts to the "curve of closure" (Fig.7) which, for $e/b = 0.28$, gives $\xi^* = 0.44 > \xi = 0.27$. In this case from Fig.7 $K_I > 0$ is found. Thus, considering the value $\xi = 0.27$ because is lower than 0.44, the final results are $\xi = 0.27$ and $e/b = 0.28$.

Finally, using the loads specified by Castigliano, by means of the evolutive analysis of the fracturing process, we obtain a crack depth at the springing extrados of the bridge arch corresponding to 27% of the depth of the section, with an axial load eccentricity at the springings $e = 0.28b = 0.56$ m.

Comparing the iterative and evolutionary analyses, it is interesting to note that the two results coincide. In fact, also Castigliano, by neglecting the effects of the mortar beds, calculated an eccentricity at the springings of 0.56 m, resulting in the formation of a 0.68 m deep crack, equal to the part of the section subjected to tension.

Vittorio Emanuele I Bridge

Vittorio Emanuele I Bridge (Fig.14) crosses Po River in Turin, joining Vittorio Veneto Square to Gran Madre di Dio Square. Vittorio Emanuele I Bridge is popularly called the "stone bridge". It consists in 5 five-centered arches, made out of Cumiana stone, and it is 150 m in length and 12 m in width.

The bridge was built during the French occupation of Turin of the early '800, under the direction of engineers Claude-Joseph La Ramée Pertinchamps and Charles-Francois Mallet from the Corps des Ponts et Chaussées of Paris. Vittorio Emanuele I Bridge was completed in 1813 (Re 1999; Re 2009).

Each five-centered arch is 25 m in span, and 8.33 m in rise. The thickness of the Cumiana stone segments is equal to 1.27 m. Vittorio Emanuele I Bridge geometry is reported in Figure 15.

Figure 14. Vittorio Emanuele I Bridge over Po River in Turin.

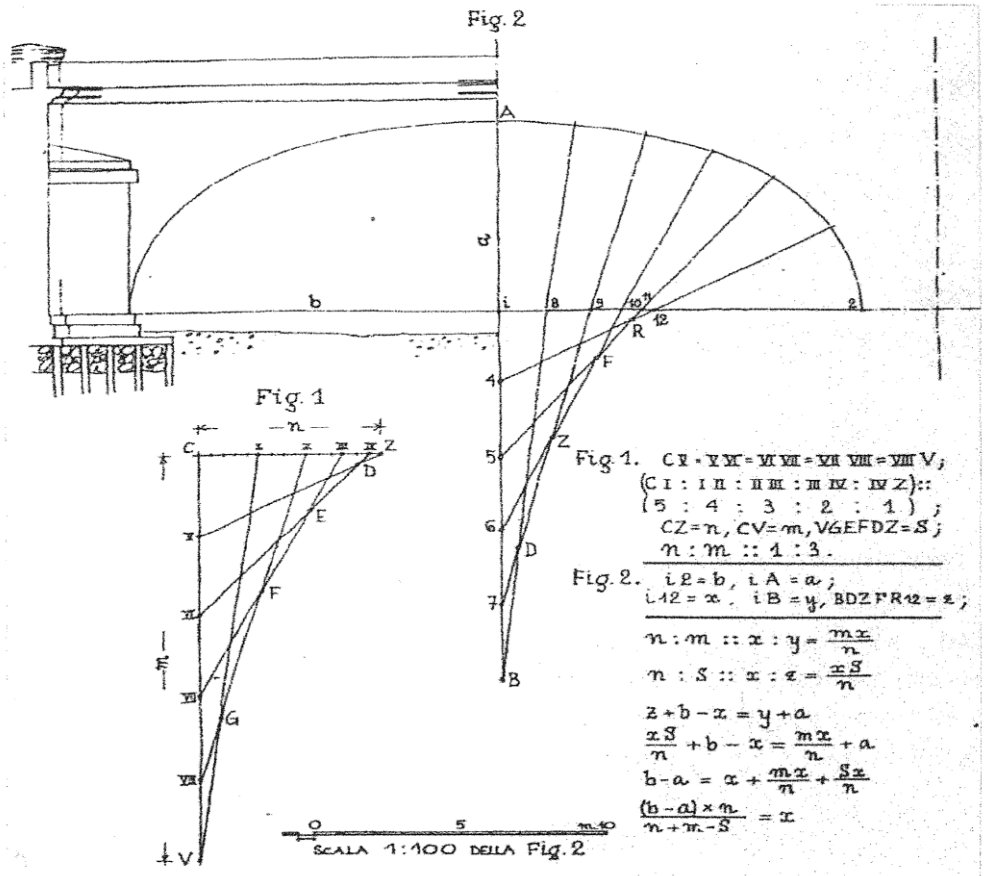

Figure 15. Polycentric Arch according to Perronet and applied to Vittorio Emanuele I Bridge (Re 2009).

Vittorio Emanuele I Bridge evolutionary analysis

With reference to the geometry described above, for a bridge stripe of unitary width, we developed a FEM model consisting of 16 beam finite elements (Fig. 16), having area $A_i = 1.27$ m^2, and moment of inertia $I_i = 0.17$ m^4 each.

The length and loads related to each segment are summarized in Table 5 (the model was seen to be symmetrical).

Table 5. Loads used in the analysis of Vittorio Emanuele I Bridge.

Voussoir	**Length**	**Segment Weight**	**Filling Weight**	**Live Load**	**Total**
	[m]	[kNm^{-1}]	[kNm^{-1}]	[kNm^{-1}]	[kNm^{-1}]
1	1.54	34.92	129.86	6.00	170.78
2	1.49	34.92	97.62	6.00	138.54
3	1.31	34.92	72.03	6.00	112.95
4	1.32	34.92	52.67	6.00	93.59
5	2.25	34.92	33.62	6.00	74.54
6	2.35	34.92	16.98	6.00	57.90
7	2.44	34.92	7.03	6.00	47.95
8	2.65	34.92	1.71	6.00	42.63

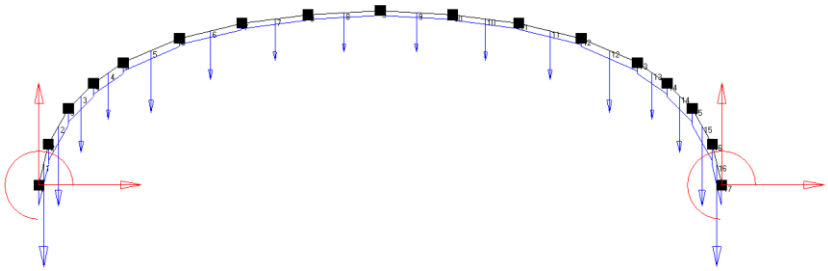

Figure 16. FEM calculation scheme of Vittorio Emanuele I Bridge.

As described above, the bridge is composed of gneiss segments (Piedmont Cumiana Stone). The system was assumed to have a compressive strength of 50 MPa, a tensile strength of 1.50 MPa, a Young's modulus of 50000 MPa, and a fracture toughness K_{IC} = 1.00 MN/m$^{3/2}$ (Bocca et al. 1989; Buyukozturk and Hearing 1998; Carpinteri 1981).

The loading process takes place in three steps, involving (i) the segments weight only, (ii) the segments weight and the filling weight, (iii) the segments weight, the filling weight and the live loads. The results are summarized in Table 6. The values refer to the sections at the haunches.

Table 6. Evolution of fracturing process in the structure of the Vittorio Emanuele I Bridge.

Step	**Load Description**	$\mathbf{F_C}$	**e**	$\mathbf{\bar{F}_C}$	**e/b**	**ξ**	**ξ***
		[kN]	[m]	[-]	[-]	[-]	[-]
i	Segments Weight	618.78	0.57	0.55	0.45	-	-
ii	Segments + Filling Weight	907.41	0.41	0.81	0.32	-	-
iii	Segments W. + Filling W. + Live Load	101373	0.42	0.90	0.33	-	-

(i) It is evident that under the segments weight alone there is no fracturing of the arch.

(ii) The application of the filling weight triggers no fracturing process at the haunches.

(iii) Moreover, by adding the live loads to the dead ones, there is no fracturing of the arch.

Finally, using the loads specified by Castigliano for Mosca Bridge analysis and considering mortar beds between stone segments, we get a very safe behaviour of the Vittorio Emanuele I Bridge structure with respect to all load increments.

CONCLUSIONS

Through a comparison with the methods traditionally used for the assessment of vaulted structures, it has been demonstrated that a more thorough analysis, which takes into account the intermediate fracturing stage of the structure (i.e., the process that takes place once the material's tensile strength has been exceeded and before the formation of the collapse mechanism), is able to provide a closer interpretation of the actual behaviour of an arch structure during its lifespan. By taking into account the damage phase that follows the elastic one, this procedure is able to overcome the conceptual shortcomings of limit analysis, in that it considers the real mechanical characteristics of the material, verifies the position of the thrust line, and takes into account the redistribution of internal stresses.

Furthermore, a description has been provided of how to carry out an evolutionary analysis of the fracturing process by drawing upon the concepts of Linear Elastic Fracture Mechanics and making use of automatic computation methods. The procedure described was applied to existing structures, Mosca Bridge and Vittorio Emanuele I Bridge, both in Turin. The results of the analysis conducted on Mosca Bridge structure were found to be consistent with the historical results obtained by Alberto Castigliano. A comparison between Mosca Bridge and Vittorio Emanuele I Bridge evolutionary analyses shows how shallow arch structures are much more sensitive to the investigated phenomena of fracture opening and closure than multi-centered arch structures.

REFERENCES

Benvenuto, E., and Radelet de Grave, P. (1995). *Between Mechanics and Architecture*, Birkhäuser, Basel.

Berto, L., Saetta, A., Scotta, R., and Vitaliani, R. (2002) "An orthotropic damage model for masonry structures", *International Journal for Numerical methods in Engineering,* 55, 127-157.

Bocca, P., Carpinteri, A., and Valente, S. (1989). "Fracture mechanics of brick masonry: Size effect and snap-back analysis." *Materials & Structures,* 22, 364-373.

Broek, D. (1984). *Elementary Engineering Fracture Mechanics*, Martinus Nijhoff Publishers, Leiden.

Buyukozturk, O., and Hearing, B. (1998). "Crack propagation in concrete composites influenced by interface fracture parameters." *International Journal of Solids and Structures*, 35, 4055-4066.

Carpinteri, A. (1981). "Static and energetic fracture parameters for rocks and concretes." *Materials & Structures*, 14, 151-162.

Carpinteri, A. (1982). "Application of fracture mechanics to concrete structures." *Journal of the Structural Division ASCE,* 108, 833-848.

Carpinteri, A. (1983). "Stiffness loss and fracture resistance of a cracked beam with circular cross section." *Meccanica*, 18, 156-162.

Carpinteri, A. (1992). *Meccanica dei Materiali e della Frattura,* Pitagora Editrice, Bologna.

Carpinteri, Al., and Carpinteri An. (1982). "Softening and fracturing process in masonry arches." *Proceedings of the 6th International Brick Masonry Conference*, Rome, 502-510.

Carpinteri, A., Invernizzi, S., and Lacidogna, G. (2007). "Structural assessment of a XVIIth century masonry vault with AE and numerical techniques." *International Journal of Architectural Heritage*, 1, 214-226.

Castigliano, A. (1879). *Théorie de l'Equilibre des Systèmes Elastiques et ses Applications*, Del Negro, Turin.

Chiorino, M. A., Icardi, A., Rolando, S., and Testa, M.. (2001). "Mechanism and finite element failure of Mosca's Bridge over the Dora in Turin." *Proceedings of the 3rd International Arch Bridges Conference ARCH'01*, Présses de l'Ecole Nationale des Ponts et Chaussées, Paris.

Chondros, T., and Dimarogonas, D. (1998). "Vibration of a cracked cantilever beam." *Journal of Vibration and Acoustics ASME,* 120, 742-746.

Choo, B. S., Coutie, M., and Gong, N. (1991). "The effect of cracks on the behavior of masonry arches." *Proceedings of the 9th International Brick/Block Masonry Conference*, Berlin, 948-955.

Crisfield, M. A., and Wills, J. (1986). "Nonlinear Analysis of Concrete and Masonry

Structures." *Finite Element Methods for Nonlinear Problems*, Springer Verlag, Berlin.
Giambanco, G., Failla, A., and Cucchiara, C. (2000). "Numerical modelling of masonry arches via interface models". *Proceedings of the* 12^{th} *International Brick/Block Masonry Conference,* Madrid, 449-463.
Heyman, J. (1966). "The stone skeleton." *International Journal of Solids and Structures*, 2, 255-296.
Heyman, J. (1969). "The safety of masonry arches." *International Journal of Mechanical Science*, 2, 363-385.
Heyman, J. (1982). *The Masonry Arch*, Ellis Horwood, Chichester.
Hillerborg, A., Modéer, M., and Petersson, P. (1976). "Analysis of crack formation and crack growth in concrete by means of fracture mechanics and finite elements." *Cement and Concrete Research*, 6, 773-782.
Invernizzi, S., Lacidogna, G., Manuello, A., and Carpinteri, A. (2011). "AE monitoring and numerical simulation of a two-span model masonry arch bridge subjected to pier scour." *Strain*, 47, 158-169.
Irwin, G. (1957). "Analysis of stresses and strains near the end of a crack traversing a plate." *Journal of Applied Mechanics*, 24, 361-364.
Karnowsky, I. (2012) *Theory of Arched Structures*, Springer.
Kooharian, A. (1953). "Limit analysis of voussoir (segmental) and concrete arches." *Journal of the American Concrete Institute*, 89, 317-328.
Krawczuk, M., Zak, A., and Ostachowicz, W. (2000). "Elastic beam finite element with a transverse elasto-plastic crack." *Finite Elements in Analysis and Design*, 34, 61-73.
Lourenço, P. (2000) "Anisotropic softening model for masonry plates and shells", *Journal of Structural Engineering ASCE*, 126, 1008-1015
Milne, I., Ritchie, R., and Karihaloo, B. (2003). *Comprehensive Structural Integrity: Fracture of Materials from Nano to Macro*, Elsevier, Amsterdam.
Murakami, Y. (1987). *Stress Intensity Factors Handbook*, Pergamon Press, Oxford.
Okamura, H., Watanabe, K., and Takano, T. (1975). "Deformation and strength of cracked member under bending moment and axial force." *Engineering Fracture Mechanics*, 7, 531-539.
Orduna, A., and Lourenço, P. (2001) "Limit analysis as a tool for the simplified assessment of ancient masonry structures." *Proceedings of Historical Construction*, Guimarães.
Page, J. (1993). *Masonry Arch Bridges*, HMSO, London.
Paradiso, M., Tempesta, G., Galassi, S., and Pugi, F. (2007) *Sistemi Voltati in Muratura. Teoria e Applicazioni*, DEI, Roma.
Parmerter, R. (1976). "A method for calculating the reduction in stress intensity factor due to an elastic foundation." *Engineering Fracture Mechanics*, 8, 539-546.

Pippard, A., and Baker, J. (1962). *The Analysis of Engineering Structures*, Edward Arnold, London.
Re, L. (1999). *I Ponti Piemontesi. Progetti e Cantieri*, Celid, Torino.
Re, L. (2009). "Il ponte napoleonico sul Po." *Progetti Integrati d'Ambito a Torino,* Celid, Torino.
Tada, H., Paris, P. C., and Irwin, G. R. (1985). *The Stress Analysis of Crack Handbook*, Paris Productions, St. Louis.
Towler, K., and Sawko, F. (1982). "Limit state behavior of brickwork arches." *Proceedings of the 6th International Brick Masonry Conference*, Rome, 422-429.
UIC Code 778-3 (1995). *Recommendations for the assessment of the load carrying capacity of existing masonry and mass-concrete arch bridges*. Paris, International Union of Railways (UIC).
Zucchini, A. and Lourenço, P. (2000) "A micro-mechanical model for the homogenization of masonry", *International Journal of Solids and Structures*, 39, 3233-3255.